Journal of Natural Sciences and Mathematics
Qassim University, Vol. 9, No. 1, pp 47-67 (January 2016/Rabi I 1437H.)

The Role of Oxidation States in Laser Light Generation and Color Image Formation of F_A: Co^{+2}, Co^{+3} Color Centers at the (001) Surface of AgBr crystal: ab initio Calculations

S. Abdel Aal

Faculty of Science, Benha University, P.O.Box 13518, Benha, Egypt, Department of Chemistry, Faculty of Science and Arts, Qassim University, P.O.Box 6666, Qassim, Buraidah, Saudia Arabia, Department of Chemistry,

E-mail: safabdelaal@yahoo.com

Abstract. The oxidation states of cobalt in F_A color center at the low coordination (001) surface of AgBr play important roles in laser light generation and color image formation. These two applications are investigated simultaneously by using quantum mechanical ab initio methods. Quantum clusters of variable sizes were embedded in the simulated Coulomb fields that closely approximate the Madelung fields of the host surface and the nearest neighbors ions to the F_A defect sites were allowed to relax to equilibrium. The calculated Stokes shifts suggest that laser light generation is sensitive to the simultaneous effects of the oxidation state of cobalt and the choice of the basis set centered on the anion vacancy. All relaxed excited states of the defect-containing surfaces were deep below the lower edges of the conduction bands of the ground state defect-free surfaces, suggesting that F_A: Co^{+2} and Co^{+3} color centers are suitable laser defects. The dependence of the orientational destruction, recording sensitivity andexciton (energy) transfer on the oxidation state of cobalt is clarified. The Glasner-Tompkins empirical rule is generalized to include the oxidation state of the impurity cation. As far as color image formation is concerned, the supersensitizer was found to increase the sensitizing capabilities of two primary dyes in the excited states by increasing the relative yield of quantum efficiency. The Co^{+3} surfaces of AgBr are significantly more sensitive than the corresponding Co^{+2} surfaces. On the basis of quasi Fermi levels, the difference in the sensitizing capabilites between the examined dyes in the excited states is determined.

Keywords:*Theoretical calculations-AgBr-F_A defects- laser -color images.*

1. Introduction

Modeling solid state processes has reached the stage at which important applications to solid state chemistry and physics would be fruitful. Theoretical modeling is an especially powerful tool that helps to design new functional materials, for it can narrow down the list of potential materials for which crystal growth techniques need to be developed. The applications of theoretical models would give benefits in testing laser light generation and color image formation. There have been very few detailed theoretical studies of the key processes for color center laser and color image formation. If such results were available, they could provide a route to new systems or to improvements in existing systems. Whilst such calculations are lacking for specific cases, there are detailed calculations for many key processes in closely related systems. In the present paper, two possible applications of the FACo+n(n=2,3) point surface defect on the AgBr (001) surface have been considered. The first application is related to its luminescence for laser applications, while the second one to the color image formation.Neither theoretical nor experimental data have been reported for the present FACo+n (n=2,3) color centers in relation to laser activity andphotographic sensitivityat the (001) surface of silver halides.

As far as laser light generation is concerned, the electron-phonon coupling provides the property of broadened Stokes-shifted optical transition bands.The electrons associated with a defect interact strongly with the surrounding vibrating crystal ions, resulting in optical transitions, which are allowed in a broad band around the defect-specific central transitions. All color center lasers realized so far are based on electronic defects**[1,2].**An *F*-center consists of an anion vacancy binding an electron. The complex F_A cenetr is an *F*center attached to a cationic impurity.The possible energy level structure of the electron at an F_A center is influenced by the shape and depth of the electronic binding potential. This potential is determined mainly by the distance and geometrical arrangement of the nearest surrounding lattice ions, which oscillate around their equilibrium positions **[3]**.

The development of color center lasers therefore depends on the testing of known color center systems with more favorable optical properties, and the development of new laser active defects. It appears that a laser-suitable defect should have the following properties: (1) one electron defect center (2) compact electronic states (3) relaxed excited states deep below the conduction band, and (4) possible experimental production of the center in high concentrations ($\geq 5\times10^{16}cm^{-3}$).

Useful F_{A2} center systems for laser applications are formed in only two host materials, KCl and RbCl [**2**]. However, *ab initio* calculations of laser light generation at the ionic crystal surface is still lacking, and until recently the potential of F_ACo^{+n} (n=2,3) center systems for useful laser action at the (001) surface of AgBr has been ignored [**4**]. A fairly extensive set of *ab initio*calculations has been carried out in an attempt to examine the role of oxidation states in laser light generation at the (001) surface of AgBr doped with Co^{+2} and Co^{+3}.Several related properties such as the relaxed excited state orientational destruction, the exciton (energy) transfer, and the Glasner-Tompkins empirical rule have also been reported.

As far as color image formation is concerned, silver halide photography contains several unique phenomena. These include characterization of silver halide micro- and macrocrystals, characterization of silver halide microclusters as latent image and sensitization centers, the relationship between electronic and molecular structure of sensitizing dyes and light induced electron transfer from sensitizing dyes to the silver halide. The traditional silver halide photographic process is still efficient in image quality for use in many applications. The unique physical properties of silver halides are responsible for their unique utility in photographic development. When a photographic film is exposed to light, on average about 8-12 absorbed photons per crystal, the photographic film is said to bear a *latent image* that is capable of being converted to a *visible image* by a developer. The formed image is either black and white or color. In the process of color image formation, electron transfer takes place from optically excited dye molecules (sensitizing dyes) to the conduction band of silver halides. Sensitizing dyes are thus required to have the abilities to absorb light at a desired wavelength and to transfer electrons from their excited states to the conduction band of silver halides. The role of irregular surface defects, such as edge or kink type defects, in latent image formation has been the subject of several investigations [5]. It has been postulated that these sites are places where a latent image cluster could preferentially form.

Despite the great advances in film quality and sensitivity, the theoretical framework describing the elementary acts of the photographic process at the atomic level has developed slowly[6-13].It is observed that less theoretical attention has been paid to the role of oxidation states at the low coordination surfaces such as (001) or electron hole centers such as $F_A$in color image sensitization. Therefore our intention to examine how electron transfer from a dye moleculeto the bottom of the conduction band of a silver chloride or bromide surface in the process of color image formation depends on the oxidation states of cobaltimpurity cation.

The present study is organized as follow: Section 2, gives a brief account of the theoretical methods, namely, simulation of the low coordination (001) surface of AgBr, configuration interaction-singles (CI-Singles), configuration coordinate diagrams (CC diagrams) and density functional theory (DFT). In Section 3, the results of the simultaneous potentials of F_A:Co^{+2} andF_A:Co^{+3}color centers in providing laser action and color image sensitizationare given and discussed. The results were then summarized and concluded.

2. Computational Details and Surface Models

2.1 Crystal simulation

There are several methods to simulate crystals, either by finite or infinite systems. For such an approach, clusters of varying sizes in the bulk structure are suitable approximations **[14-21].**A finite ionic crystal of 288 point charges was first constructed. The Coulomb potentials along the X and Y axes of this crystal are zero by symmetry as in the host crystal. The ±1 charges on the outer shells listed in **Table 1**, were then modified, by using a fitting procedure, to make the Coulomb potential at the four central sites closely approximates the Madelung potential of the

host crystal, and to make the Coulomb potential at the eight points with coordinates (0,±R,±R) and (±R,0,±R) where R is half the lattice distance, which for AgBr is 2.887 Aº, equal to zero as it should be in the host crystal. With these charges, 0.409283 and 0.800909, the Coulomb potential in the region occupied by the central ions is very close to that in the unit cell of the host crystal. The Coulomb potential was calculated to be (1.748) at the four central sites (compared with 1.746 for a simple cubic ionic crystal) and (0.0) at the previously defined eight points (compared with 0.0 for the same crystal),**Fig.1**.

Table 1. Specification of the finite lattices used for the (001) surfaces of AgBr. R is half the lattice distance, which for AgBr is 2.887 Å and r, is the distance of the appropriate shell from the center of the lattice.

	Bulk		(001)		
r^2/R^2	Coordinates/R (±X), (±Y), (±Z)	Number of centers	Coordinates/R (±X), (±Y), (Z≤0)	Number of centers	Charge | q |
2	1 1 0	4	1 1 0	4	1
6	1 1 2	8	1 1 2	4	1
10	3 1 0	8	3 1 0	8	1
14	3 1 2	16	3 1 2	8	1
18	1 1 4	8	1 1 4	4	1
18	3 3 0	4	3 3 0	4	1
22	3 3 2	8	3 3 2	4	1
26	5 1 0	8	5 1 0	8	1
26	3 1 4	16	3 1 4	8	1
30	5 1 2	16	5 1 2	8	1
34	3 3 4	8	3 3 4	4	1
34	5 3 0	8	5 3 0	8	1
38	5 3 2	16	5 3 2	8	1
38	1 1 6	8	1 1 6	4	1
42	5 1 4	16	5 1 4	8	1
46	3 1 6	16	3 1 6	8	1
50	5 5 0	4	5 5 0	4	1
50	5 3 4	16	5 3 4	8	1
50	7 1 0	8	7 1 0	8	1
54	5 5 2	8	5 5 2	4	1
54	3 3 6	8	3 3 6	4	1
58	7 3 0	8	7 3 0	8	1
66	5 5 4	8	5 5 4	4	1
54	7 1 2	16	7 1 2	8	0.409293
62	7 3 2	16	7 3 2	8	0.409293
66	1 1 8	8	1 1 8	4	0.800909
82	9 1 0	8	9 1 0	8	0.800909
86	9 1 2	16	9 1 2	8	0.800909

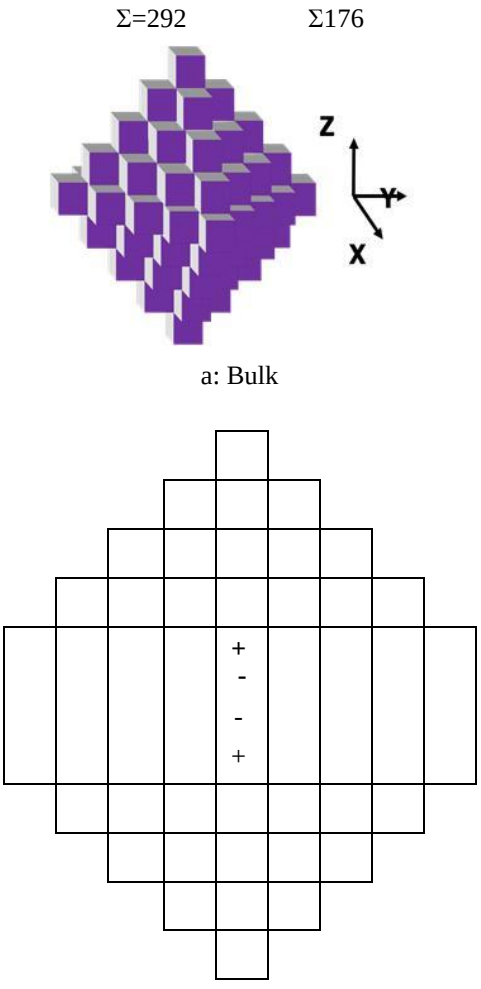

Fig.1: Z = 0 plane representations of the AgBr crystal considered in the calculations.
a: Bulk b: (001)

All charged centers with Cartesian coordinates (±X), (±Y) and (Z>0) were eliminated to generate the (001) surface with 176 charged centers occupying the three dimensional space (±X), (±Y) and (Z≤0). The clusters of **Fig.2** were then embedded within the central region of the crystal surface. All the electrons of the embedded clusters were included in the Hamiltonian**s** of the *ab initio* calculations. Other crystal sites entered the Hamiltonian**s** either as full or partial ionic charges as demonstrated in **Table 1**.

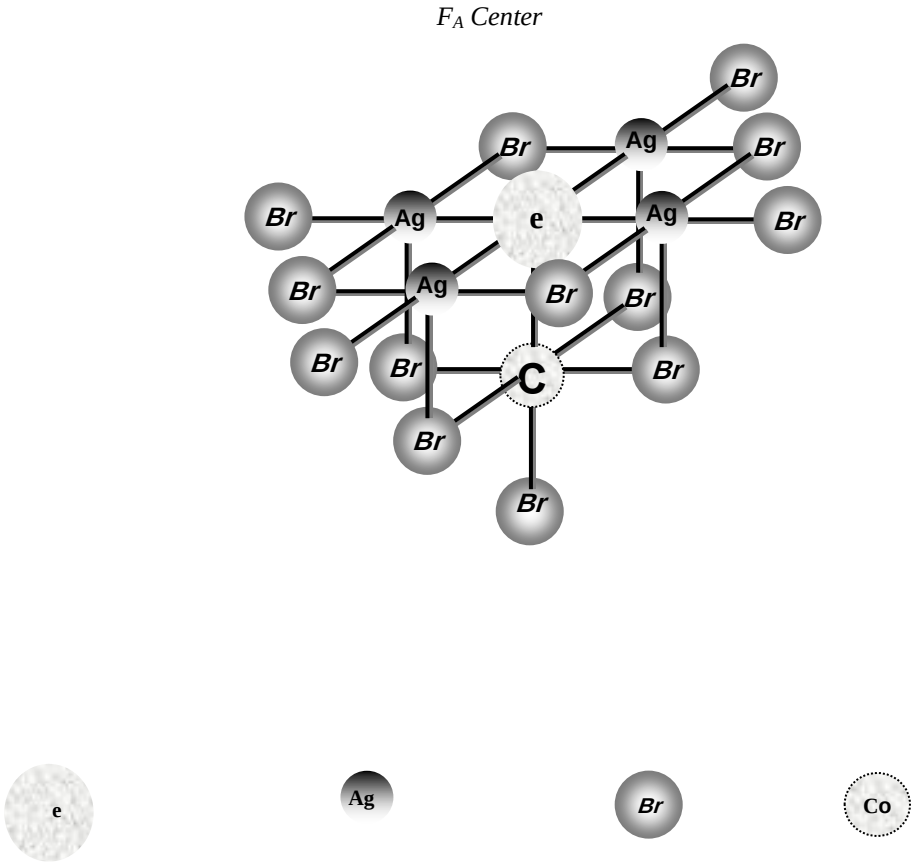

Fig. 2:The low coordination surface cluster which are considered in the calculations.

2.2 Configuration Coordinate diagrams

To construct the configuration coordinate diagrams, the ion clusters representing the F_A centers at the (001) surfaces of AgBr were first embedded in the three-dimensional arrays of the point-ions that have been described in section 2.1 The representations of the ion clusters considered in the present calculations are given in **Fig.2**. The absorption and emission energies were then calculated as the difference between the total energies of the ground- and excited- states. For this purpose, the relevant potential energy curves were calculated, then according to the

Franck-Condon principle the absorption energy was calculated as that for a vertical transition from the minimum of the relaxed ground state to the excited state. The fluorescence energy was calculated in a similar manner. Stokes shifts were then calculated as the difference between absorption and emission energies.

$$\Delta E_{absorption} - \Delta E_{emission.} \quad (1)$$

2.3 Configuration Interaction-Singles method

The configuration interaction-singles method was employed for the calculations of $F_A$laser activity, exciton (energy) transfer, relaxed excited state orientational destruction of the F_A center and reorientational efficiency. The method includes some electron correlation in the excited states **[22a]**, and can provide reasonable accuracy for excitation energies in comparison with the simplest way to find the lowest relaxed excited state in wide gap insulators, namely, the self consistent field calculations of the triplet state **[23]**. It is observed that Sousa and Illas**[22b]**have examined the impact that proper electron correlation treatment could have optical absorption energy of *F*-centers in MgO.

2.4 Density Functional Theory method

Density functional theory method was employed for the calculations of the differences between the band gaps, exciton bands and color image formation. The calculations were performed by using Becke's three-parameter exchange functional B3 with LYP correlation functional [**24**]. This hybrid functional includes a mixture of a Hartree-Fock exchange with DFT exchange correlation. Originally the functional B included the Slater exchange along with corrections involving the gradient of the density [**25**] and the correlation functional LYP is that of Lee, Yang and Parr, which includes both local and non-local terms [**26**].It may be worthnoting that the drawback of the density functional theoy to prdict the excitation energies of charge transfer states and to give the exact long range 1/R dependance on donor-acceptor distance is due to the local character of theapproximate exchange-correlation functionals. In other words, long range charge transfer excited states in the time-dependant density functional theory require non local exchange.

2.5 Compact Effective Potential basis sets

The Stevens, Basch and Krauss Compact Effective Potential CEP basis sets [**27**] were employed in the present calculations. In these CEP basis sets, the double zeta calculations are referred to as CEP-31G, and similarly triple zeta calculationsto as CEP-121G. It may be noted that there is only one CEP basis set defined beyond thesecond row,and the two basis setsareequivalent for these atoms.These basis setshavebeen used to calculate the equilibrium structure and spectroscopic properties of several molecules, and the results compared favorably with corresponding all-electron calculations. The computations reported in this paper were carried out by

using Gaussian 09 system [**28**].The figures were generated by using the corresponding Gauss View software.

3. Results and Discussion

3.1 $F_A$laser and related optical properties

3.1.1 F_A laser

The configuration coordinate data ofF_A centers at the low coordination (001) surface of AgBr are given in **Table 2**, and the configuration coordinate curves are shown in **Fig.3**. Since the electron density localization in the vacancy is an important feature of a defect with potential laser applications, the optical absorption and fluorescence energies after adding Br functions on the anion vacancy of AgBr have been calculated.The results that collected in **Table 2** and **Fig.3**, suggest that laser light generation is sensitive to the simultaneous effects of the oxidation state of the impurity cationand the choice of the basis set centered on the anion vacancy**.** Greater Stokes shifts are assigned to the oxidation state Co^{+3} relative to the oxidation state Co^{+2}.

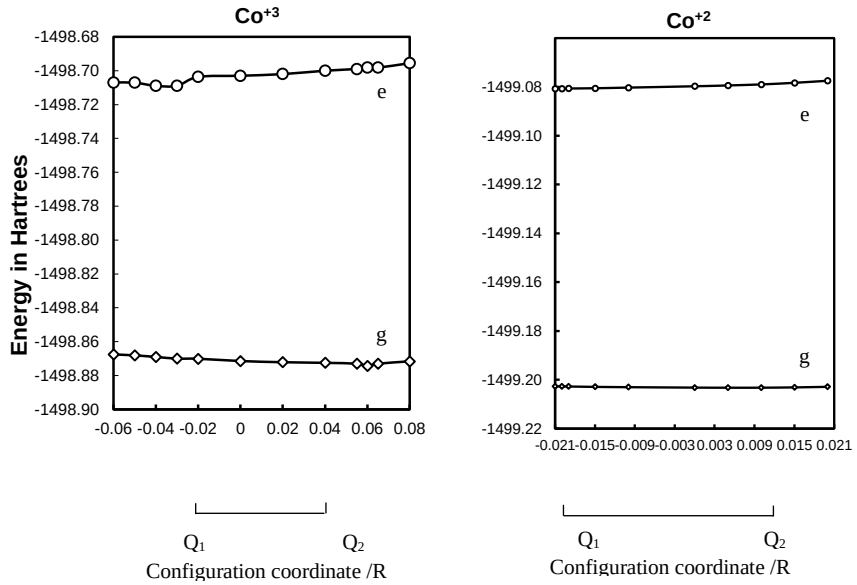

Fig. 3: The configuration coordinate diagrams of the (001) low coordination surface of AgBr. Q_1: Minima of the ground state Q_2: low lying excited states

Table (2): The effect of the, dopant, on minima of the ground states (Q_1) and low lying excited states (Q_2), horizontal shifts along the configurations coordinate $|Q_2-Q_1|$, absorbed and emission transition energies ΔE between the ground states (g) and the low lying excited states (e) of F_A centers at the low coordinated (001) surface of AgBr, calculated at the CIS level. R=2.887 Å, and energies in eV.

Crystal	Surface	Dopant	Q_1/R	Q_2/R	$\|Q_2-Q_1\|/R$	$\Delta E_{absorption}$	$\Delta E_{emission}$	Stokes-Shift
AgBr	001	Co^{+3}	0.022	-	0.057	4.685	4.465	0.219
			0.03	0.035	0.03	4.599	4.705	0.106*
				0.00				
		Co^{+2}	0.009	-	0.03	3.379	3.318	0.061
			-0.01	0.021	0.01	3.331	3.087	0.023*
				-0.02				

* CEP-121G basis functions of Bromine are added to the Bromine vacancy.

A laser-suitable defect should have relaxed excited states deep below the conduction band of the perfect crystal [4]. To examine this issue, the band structure of AgBr surfaces, i.e, the positions of the one- electron defect levels with respect to the perfect surface bandshas been considered. In Table 3, the tops of the valence bands and the bottoms of the conduction bands for the ground states of the defect free surfaces as well as the highest occupied molecular orbitals and the lowest unoccupied molecular orbitals for the relaxed excited states of the defect containing surfaces have been collected. As shown, all excited states are below the lower edges of the conduction bands of the defect free surfaces implying that F_A could be laser suitable defect.

Table (3): The tops of valence bands (VBs) and the bottoms of the conduction bands (CBs) of the defect free surfaces in the ground states, and the highest occupied molecular orbitals (HOMOs) and the lowest unoccupied molecular orbitals (LUMOs or defect levels) of the defect containing surfaces in the relaxed excited states, calculated at the CIS level. Energies are given in eV.

Crystal	surface	Defect free surfaces ground state		Defect containing surfaces relaxed excited state		
		VBs	CBs	dopant	HOMOs	LUMOs
AgBr	001	-9.98	1.094	Co^{+3}	-15.541	-7.469
				Co^{+2}	-12.713	-3.550

3.1.2. Relaxed excited state orientational destruction

One consequence of the relaxed excited state saddle point-ion configuration of F_A center is a temperature-independent ionic-reorientation during the pump cycle, i.e, a change of the center axis into a perpendicular (equivalent) orientation. This effect can be understood from **Fig.4** where it is seen that after the emission process the assumed saddle point ion has a 50% chance of hopping to the <110> anion vacancy site opposite to its starting location. The F_A- center system may be excited in either one of its absorption bands with polarized light having its propagation direction parallel to a <001> axis and the electric field vector E parallel to a perpendicular <001> axis. Then the F_A centers excited by this E-vector will quickly be reoriented to <001> directions where the F_A centers are no longer excited and this reoriented system will become experimentally transparent for the excitation light **[2]**. However, it has been investigated experimentally and theoretically by many workers that any spectrum regions in the F_A- band absorption range is not completely transparent even after prolonged preferential optical-excitation of F_A centers[2, 29a].

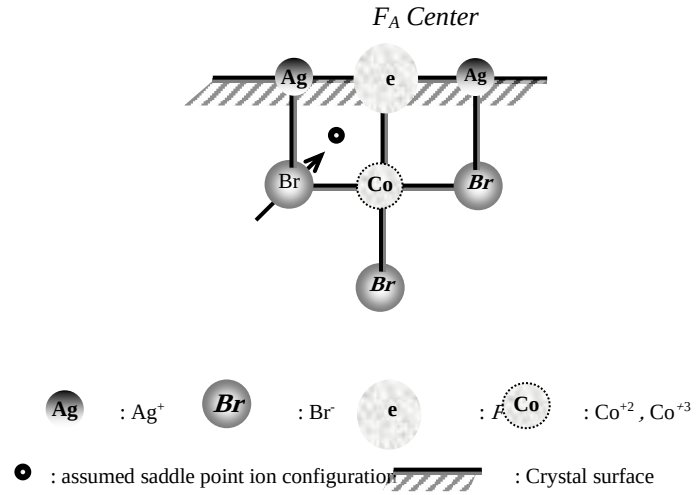

Fig. 4: Representation of the assumed relaxed excited state saddle-point ion configuration responsible for the orientational destruction of the F_A center in laser experiment.

To examine theoretically the relaxed excited state orientational destruction of the F_A center, the total energies of the original relaxed excited state ion configuration and the assumed saddle point ion configurations of F_A centerat the low coordination (001) surface of AgBrhave been calculted. The differences between the energies of

these configurations (the energy barriers to the orientational bleaching in laser experiment) are given in **Table 4**. The energy barrier to the migration of the anion species to the F_A vacancy sitesincrease as the oxidation state increases.It turns out that the orientaional destruction of F_A:Co^{+2}center is more probable than that of F_A:Co^{+3}center. Experimentally, in order to avoid the orientational bleaching, the pump polarization and direction of propagation of the pump beam inside the crystal have to be chosen such that they are not parallel to a <001> direction.

Table (4): The energy barriers to the orientational destruction of F_A centers at the low coordination surfaces of AgBr due to the migration of the bulk anion to the assumed saddle point ion configurations, calculated at the CIS level. Energies are given in eV.

AgBr	001	Co^{+3}	8.016
		Co^{+2}	3.482

3.1.3 Reorientation efficiency and optical memories

It is possible to use the reorientation properties of such defects as $F_A$centers, under the action of polarized light to store information [**3**]. F_A centers could reorient easily at relatively low temperatures, and above 140 K, the reorientation efficiency is very high, which implies a high recording sensitivity. However, at 55 K this efficiency practically vanishes; thus it is possible to "read" with polarized light. Finally, in the dark, there is no thermal reorientation of the centers, and thus the information may be stored indefinitely. As shown in **Table 4**, the reorientation efficiency (probability) of F_A centers due to the migration of the bulk anions to the assumed saddle-point ion configuration of **Fig.4**decrease as the oxidation state of the impurity cation increases.This implies a high recording sensitivity for F_A:Co^{+2}center relative to that F_A:Co^{+3}.

3.1.4. Exciton (energy) transfer

The relative total energies of the excited states at different low coordination surface sites could be used as the first indicator of whether the exciton excited at a particular surface site will transfer to another site. relative energies of the excited states were estimated following the method of Shluger et al. [**23**]. As can be seen from **Fig.5**, the relative energies of F_A:Co^{+2}were less negative than those ofF_A:Co^{+3} at the (001) surface. In other words the relative energies at the low-coordination (001) surface sites of AgBr are sensitive to the $F_A$imperfection, and there is a possibility for exciton transfer from the F_A:Co^{+2} to F_A:Co^{+3} surface sites. Cox and Williams [**29**] argued that the excited state at the surface have positive values. Our estimates suggest that it could have negative values in agreement with the estimates of Shluger et al.[**23**] for MgO.

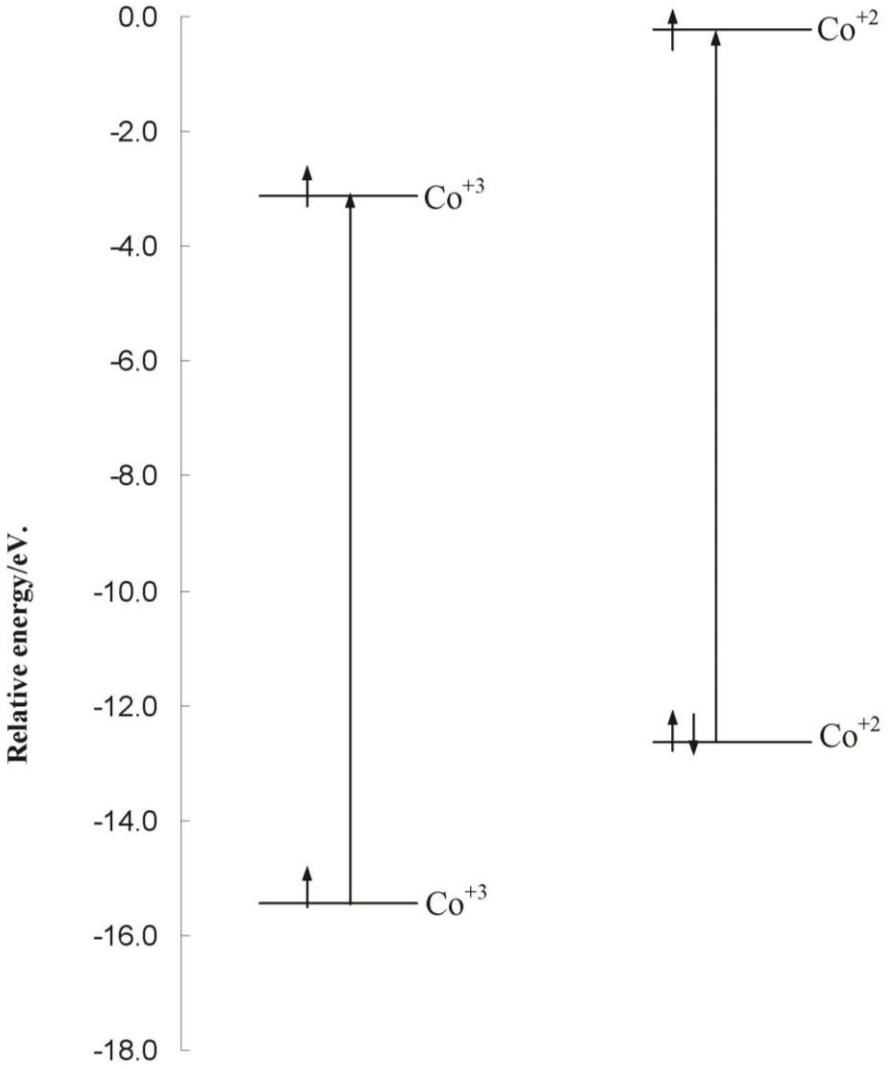

Fig. 5: Diagram representing the relative energies of the ground and exited states of the low coordinated (001) surface of AgBr, calculated at the CIS level.

3.1.5 Glasner -Tompkins relation

To apply the Glasner-Tompkins relation [**30-34]** to the present F_A centers, the corresponding band gaps and exciton bands have been calculated. The simple electron transfer model of the fundamental optical absorption of ionic solids developed by Hilsch and Pohl[**35**]has been used. Therefore,the calculated exciton band E_X as the change in Coulomb energy, associated with the transfer of an electron from a halide anion to a silver cation, both placed adjacent to the F_A center, and calculated the band gap E_{FA} as the energy difference between the highest occupied molecular orbital and the lowest unoccupied molecular orbital energy levels. The correlation between the surface ion coordination, the F_A center and the energy difference between the exciton bands E_X and band gaps E_{FA} are given in **Table 5**. As one can see from **Table 5**, the energy difference increases as the oxidation state of the impurity cation decreases. This suggests that the difference between the first exciton absorption energy E_X and the *F* band energy E_F does not depend only on the negative ion species, but also on the oxidation state of the positive ion species.

Table (5): $F_A$band gap $E_{FA}$and exciton bands E_X at the defect containing surfaces of AgBr calculated at the DFT level. Energies are given in e.V.

			E_{FA}	E_X	$E_X - E_{FA}$
AgBr	001	Co^{+3}	0.029	10.518	10.489
		Co^{+2}	0.227	11.121	10.895

3.2 Color image formation

By far the majority of practical sensitizing dyes are of cyanine or merocyanine classes, consisting of a conjugated carbon chain linking cyclic end groups. In the ground states of such a molecule, the highest occupied molecular orbital HOMO is filled, and absorption of light promotes an electron to the lowest unoccupied molecular orbital LUMO, usually in a $\pi \rightarrow \pi^*$ transition. The involved energy levels are dependent on molecular structure, and most of the relationships are now well understood**[36-45]**.

It may be noted that the evaluation of the electronic structure of dyes with respect to the silver halide surface suffers from sub-estimation of band gaps, as typical for the DFT methods. In general, the origin of the DFT drawback in describing the electronic structure of charge transfer materials seems unfortunately not be well understood. However, this does not need to ruin the relative comparison between dyes, but affects the absolute results. Moreover, the image sensitization takes place upon adsorption of a dye on the surface of silver halide crystal. Due to

the interaction between the dye and the silver halide crystal , the electronic properties of the dye/silver halide adduct will be to a certain extent different from those of the isolated species. The adsorption effects should be taken into account. However, it is known that the adsorptivity of sensitizing dyes to silver halides varies to a large extent **[14,17,46]**. The heats of adsorption of sensitizing dyes to silver halides were ca. 10 Kcal/mole, where gelatin tends to reduce the rate of heat of dye adsorption. It is also judged from experimental results that the interaction between cyanine dyes and silver halides is physical in nature and is based on the van der Waals and Coulombic forces.

3.2.1 Supersensitization

Supersensitization may be defined as a phenomenon in which the relative quantum yield of spectral sensitization Φ of a primary dye (electron acceptor) is increased on addition of a secondary dye (electron donor) called a supersensitizer SS.

To examine the effect of supersensitizer, full geometry optimizations for two dye molecules at the semi empirical level of theory using Hamilitonian **[47]**have been carried out. The optimal geometries were then used as input data for the density functional theory DFT/B3LYP calculations employing the CEP basis set. Using the DFT level of theory, the top of the valence band VB and the bottom of the conduction band CB of the defect-free surface as well as the HOMOs and LUMOs of the defect containing surfaces were calculated. The skeletal representation of the two dye- molecules 1 and 2 are shown in **Fig.6**

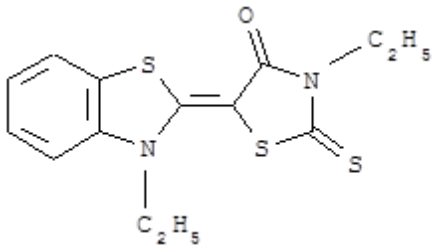

Dye 1

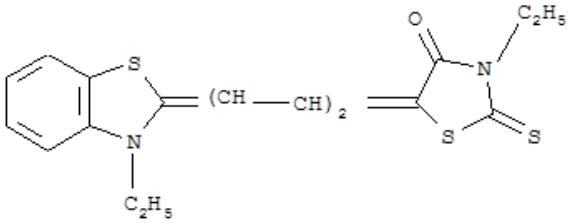

Dye 2

Fig. 6a: The skeletal forms of the sensitizing dyes 1 and 2, which are considered in the calculations.

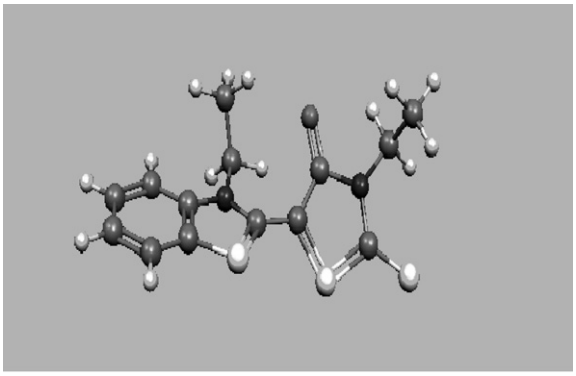

Dye - 1

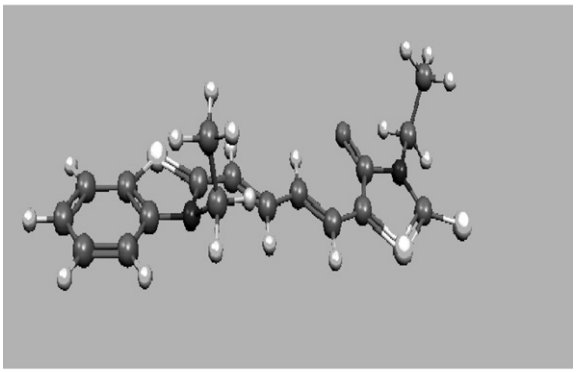

Dye - 2

Fig. 6b: Optimal configurations of Dye 1 and Dye 2. which are considered in the calculations.

The electronic energy level diagram showing hole-trapping supersensitization of Dyes 1 and 2 by a supersensitizer SS is given in **Fig.7.** In **Fig.7**, Dye* and Dye^- are Dyes in the lowest singlet excited state and in the one-electron surplus state, respectively. The top of the valence band VB and the bottom of the conduction band CB of the defect-free surface of AgBr as well as the HOMOs and LUMOs of the defect containing surfaces, are shown together with the α- and β- spin states of each Dye^-. As can be seen from **Fig.7**that the supersensitizer SS increased the sensitizing capabilities of Dyes 1 and 2 by increasing the relative yield of quantum efficiency Φ at the low coordination (001) surface of AgBr.Wheras the F_A:Co^{+2}center did not increase the relevant sensitizing capabilities because the LUMOs of the defect containing surfaces were not lowered relative to the bottoms of the conduction bands of the defect free surfaces. However, the F_A:Co^{+3} centers increased the relevant sensitizing capabilities because the LUMOs of the defect containing surfaces were

lowered relative to the bottoms of the conduction bands of the defect free surfaces. This implies that the higher oxidation state of cobalt was associated with a significant increase in the photographic sensitivity of the AgBr thin film.

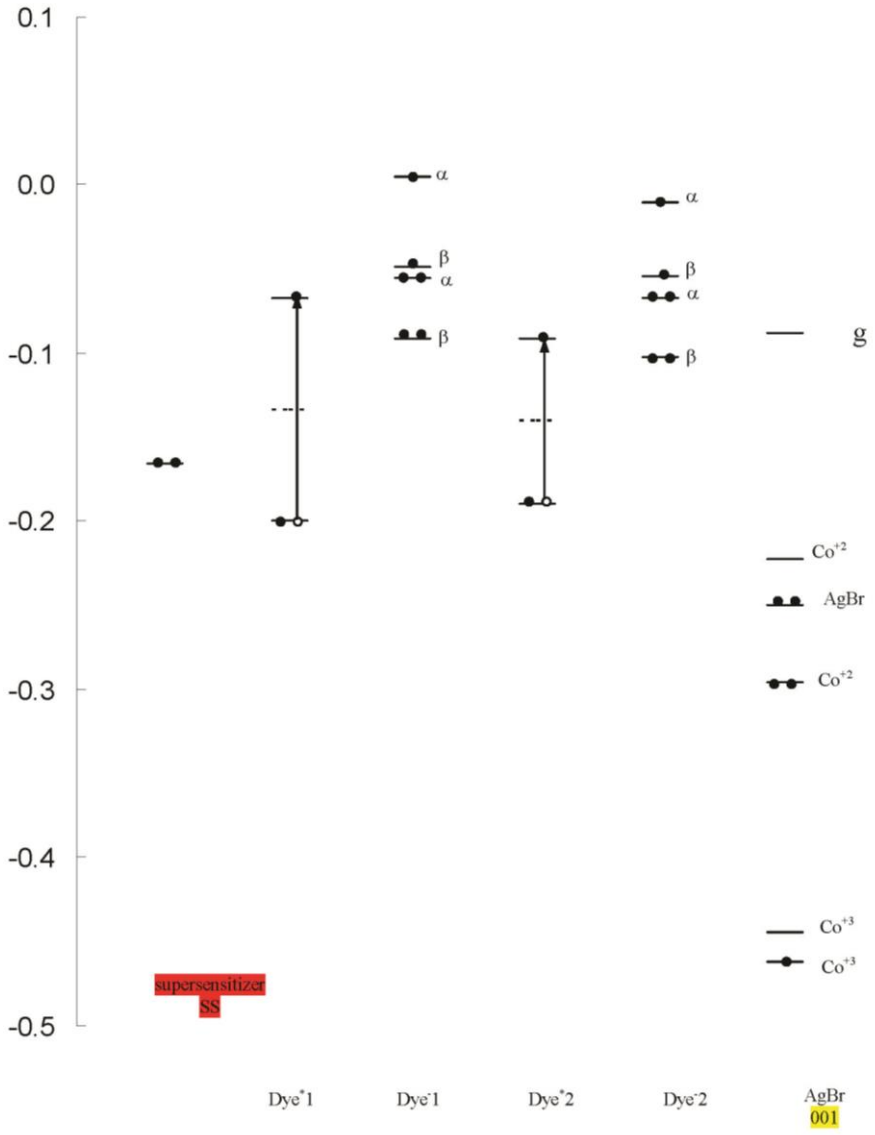

Fig. 7: The electronic energy level diagram of the dye molecules and silver halide molecules.

3.2.2 Quasi Fermi levels and sensitizing capabilities

As shown in Fig.7, the highest occupied molecular orbitals of Dyes 1 and 2 lie above the tops of the valence bands of the defect free surfaces. This implies that hole trapping desensitization is not allowed. The lowest singly occupied molecular orbitals of Dyes 1 and 2 lie above the bottoms of the conduction bands of the defect free surfaces. This in turn implies that electron transfer sensitization is allowed for Dyes 1 and 2. To determine quantitatively the difference in the sensitizing capabilities between Dye 1 and 2, the quasi Fermi levels from the relation **[48]**have been calculated.

$$[E_{HOMO} + E_{LUMO}]/2 \qquad (5)$$

Quasi Fermi levels were calculated to be 0.1323 Hartreesfor Dye 1 and 0.1396 Hartrees for Dye 2. This in turn confirms that Dye 1 has greater sensitizing capability than that of Dye 2.

Conclusions

Ab initio molecular electronic structure calculations have been carried out to examine the role of oxidation states in two practically important applications ,namely, laser light generation and color image formationat the low-coordination (001) surfaceof AgBr. Two commonly used methods namely, CIS and DFT, have been employed in the calculations, and quantum clusters have been embedded in the simulated Coulomb fields of the crystal surface. Relaxations to equilibria were taken into account, and the CEP-121G basis set was employed in the calculations. The considered F_A: Co^{+2} , Co^{+3}color centers were found to be suitable laser defect, and laser activity was found to increase as the oxidation state of cobalt ion increases. A high recording sensitivity for F_A:$Co^{+3}$was assigned relative to F_A:Co^{+2}.Exciton (energy) transfer took place from the (001) surface to the (110) surface. The Glasner– Tompkins relation was generalized to include the oxidation state of ion species. Greater sensitizing capabilities were assigned to Dye 1 relative to dye 2and the oxidation state of the impurity cation increases.The potentials of the examined color centers have been clarified, and the search for other potential defects in silver- or alkai- halides is suggested for future investigations.

References

[1] W.B. Fowler, Physics of Color Centers, Academic Press, New York (1968).

[2] W.Gellermann, J.Phys. and Chem.Solids 52(1991) 249 and references therein. S.Glaus and G.Calzaferri and R.Hoffmann, Chem.Eur.J. 8(2002)1785. S.Glaus and G.Calzaferri, Photochem. and Photobiol. Sci. 2(2003)398.

[3] D.B.Fitchen, Physics of Color Centers (Edited by W.B Fowler), Chap.5. Academic Press, New York (1968).

[4] A.S.Shalabi, T.F.El-Essawy, M.M.Assem and S.Abdel-Aal, J.Phys. and Chem. Solids 63(2002)749. A.S.Shalabi, M.E.Nour, A.M.Morsi and W.A.Zordoc, **Curr.Appl.Phys. 1(2001)427.**

[5] L.E.Brady and J.F.Hamilton, J.Appl.Phys., 37(1966)2268. **R.C.Baetzold, J.Phys.Chem.B 101(1997)8180.**

[6]J.F.Hamilton, Adv. in Phys., 37(1988)359.

[7] J.Flad, H.Stoll, A.Nicklass and H.Preuss, Z.Phys.D 15(1990)79.

[8] K.B.Shelimov, A.A.Safonov and A.A.Bagatur'yants, Chem.Phys.Lett., 84 (1993)201.

[9] T.Tani, "*Photographic Sensitivity : Theory and Mechanisms"*, Oxford University Press, New York (1995)

[10] Abds-Sami Malik, John T.Blair, William A.Bernet, Francis J.DiSalvo and Roald Hoffman, J.Solid State Chem., 146(1999)516.

[11] R.K.Hailstone, J.Appl.Phys., 80(1999)1363.

[12] A.S.Shalabi and Kh.M.Eid, J.Mol..Mod. 7(2001) 216.

[13] a.A.S.Shalabi, J.Comput.Chem. 23(2002)1104.b.A.S.Shalabi, I.A.Z.Alansari, K.Kh.Al-Naimi, M.A.Kamel, A.M.El-Mahdy, H.O.Taha and M.M.Shalaby, Phys.Chem.Chem.Phys. 6 (2004) 626.

[14] A.S. Shalabi, S. Abdel Aal, W.S. Abdel Halim, Comput. Mater. Sci., 38 (2006) 144.

[15] E.A.Colborn and W.C.Mackrodt, Surf.Sci., 117(1982)571.

[16] Z.Barandiaran and L.Seijo, J.Chem.Phys., 89(1988)5739. Z.Barandiaran and L.Seijo, in " *Computational Chemistry:Structure, Interactions and Reactivity",* Vol.77B of " *Studies in Physical and heoretical Chemistry*", edited by S.Fraga (Elsevier:Amsterdam) pp. 435-481,1992.

[17]A.S. Shalabi, M.A. Kamel, H.Y. Ammar, W.S. Abdel Halim, S. AbdlAal, J. Mol. Struc.: THEOCHEM 755 (2005) 221.

[18] E.A.Colbourn, in: C.R.A.Catlow (Ed.), " *Advances in Solid State Chemistry*", Vol. I. JAI Press, London, 1999.

[19]a. A.S.Shalabi, A.M.El-Mahdy, M.A.Kamel and H.Y.Ammar, Phys.B., 292 (2000) 59. b. A.S.Shalabi, Kh.M.Eid, M.A.Kamel and Z.M.Fathi, I.J.Modern Phys.C 11(2001)1491.

[20] A.S.Shalabi, A.M.El-Mahdy, M.A.Kamel and G.H.Ismail, J.Phys. and Chem. Solids, 60 (2001) 1007. A.S.Shalabi, A.M.El-Mahdy, M.A.Kamel and H.Y.Ammar, Phys.B., 304 (2001) 444

[21] A.S.Shalabi and A.M.El-Mahdy, J.Phys. and Chem.Solids, 60 (1999) 305. A.S.Shalabi and A.M.El-Mahdy, Phys.Lett.A 281(2001)176.

[22] a. J.B.Foresman, M.Head-Gordon, J.A.Pople and M.J.Frisch, J.Phys.Chem. 96(1992)135. J.B.Foresman and J.B.Foresman, Exploring Chemistry with Electronic Structure Methods, 2nd edition (Gaussian Inc., Pittsburgh, PA,1996). b. C.Sousa and F.Illas, J.Chem.Phys.,115(2001)1435. c.W.Kohn and L.J.Sham, Phys.Rev.A, 140(1965)1133.

[23] A.L.Shluger, P.V.Sushko and L.N.Kantorovich, Phys.Rev.B 59(1999)2417.

[24] A.D.Becke, J.Chem.Phys. 98(1993) 5648.

[25] A.D.Becke, Phys.Rev.A 38(1988) 3098.

[26] C.Lee, W. Yang and R.g.Parr, Phys.Rev.B 37 (1988) 785. B.Miehlich, A.Savin, H.Stoll and H.Preuss, Chem. Phys.Lett.157 (1989) 200.

[27] W.Stevens, H.Basch and J.Krauss, J.Chem.Phys. 81(1984)6026. W.Stevens, M.Krauss, H.Basch and P.G.Jasien, Can. J.Chem.70(1992) 612. T.R.Cundari and W.J. Stevens, J.Chem.Phys. 98(1993)5555.

[28] M.J. Frisch et. al (2009) Gaussian 09. Gaussian Inc, Pittsburgh, PA.

[29] a. T. B.Tang, K. Seki, H. Inokuchi, T. Tani, J Appl Phys 59 (1986), 5. b. A.Cox and A.A.Williams, Surf.Sci., 175(1986)782.

[30] Glasner and F.C.Tompkins, J.Chem.Phys. 21(1953)1817.

[31] M.S.Malghani and D.Y.Smith, Bull.Am.Phys.Soc., 36(1991)1681. M.S.Malghani and D.Y.Smith, J.Phys. and Chem.Solids, 53(1992)831.

[32] A.S.Shalabi, A.M.El-Mahdy, Kh.M.Eid. M.A.Kamel and A.A.El- Barbary, Phys.Rev.B 60(1999)9377.

[33] A.S.Shalabi, T.F.El-Essawy, M.M.Assem and S.Abdel-Aal, Curr.Appl.Phys. 2(2002)97. A.S.Shalabi, T.F.El-Essawy, M.M.Assem and S.Abdel-Aal, Physica B 315(2002)13.

[34] R.S.Knox, " Theory of excitons", Academic Press, New York,1963. V.G.Plekhanov, Phys.Rev.B 54(1996)3869. A.A.O.Connel-Bronin, Phys.Stat.Sol., 38(1996)1489. G.F.Koster and J.C.Slater, Phys.Rev. 95(1954)1167; 96(1954)1208. J.H.Crawford and L.M.Slifkin(Eds.), " *Point defects in Solids*", Plenum, N.Y., 1972. W.Hayes and A.A.Stoneham, " *Defects and Defect Processes in Non-Metallic Solids* ", Wiley, New York, 1985. E.Kotomin, A.Popov, Nucl.Inst.Meth.B 141(1998)1 and references therein.

[35] R.Hilsch and R.W.Pohl, Z.Phys., 57(1929)145; 59(1930)812.

[36] W.West, P.B.Gilman, in" *The theory of Photographic Sensitivity*" Fourth edition,, T.H.James edition, Macmillan, New York (1977) Chap. 10.

[37] T.Tani, J.Imaging Sci., 34(1990)143

[38] R.W.Gurney, N.F.Mott, Proc.R.Soc. London Ser. A,146,151 (1938).

[39] Tamura and H.Hada, Photogr.Sci.Eng. 11(1967)82. T.Tani and S.Kikuchi, Photogr.Sci.Eng. 11(1967)129; T.Tani, ibid., 13(1969)231; ibid., 14((1970)63; T.Tani, S.Kikuchi and K.Honda, ibid., 12(1968)80.

[40] L. Kong, Z. Jiang, H.H. Lai, R.J. Nicholls, T. Xiao, J. Catal., 293(2012) 116.

[41] R.Large, "Photographic Sensitivity" edited by R.Cox, Academic Press, New York(1973).

[42]R.C.Nelsonand P.Yianoulis, Photogr.Sci.Eng. 22(1978) 2.

[43] E.Moisar and F.Granzer, Photogr.Sci.Eng., 26(1982)1. J.F.Hamilton and R.C.Baetzold, Photogr.Sci.Eng., 25(1981)189.

[44] R.C.Baetzold, Photogr.Sci.Eng., 17(1973)78; ibid., 19(1975)11; ibid., 28(1980)15. L.Francois, M.Mostafavi,J.Belloni,J.F.Deluois and J.Delaire, J.Phys.Chem. 26(2000)6133. L.Francois, M.Mostafavi,J.Belloni and J.Delaire, Phys.Chem.Chem.Phys. 3(2001)4965.

[45]a. A.Dreuw, J.L.Weisman, M.Head-Gordon, 119(2003)2943. P.B.Gilman, J.Photogr.Sci.Eng., 18(74)418.

[46]T.Tani, T.Suzomoto, K.Ohzeki, J.Phys.Chem., 94(1990)1298.

[47]M.J.S.Dewar and C.H.Reynolds, J.Comp.Chem., 2(1986)140.

[48]T.Tani, Photogr.Sci.Eng., 18(1974)165.

" دور حالات التأكسد في توليد ضوء الليزر و تكوين الصور الملونة للمراكز اللونية FA: Co+2, Co+3 على سطح بلورة بروميد الفضة (001): باستخدام حسابات آب إينيشيو"

صفاء عبدالعال

ملخص البحث. صمم هذا البحث لإجراء دراسة مقارنة لدور حالات التأكسد للأيون الكوبلت الشائب للمراكز اللونيةF_A: Co^{+2}, Co^{+3} على كل من توليد ضوء الليزر و تكوين الصور الملونة و التداخلات بين السطح الماز و الجسيمات الممتزة علي سطح بلورة بروميد الفضة والموصوفة بمعاملات ميلر(001).ذلك باستخدام نظرية دالة الكثافة (DFT) و نموذج العناقيد المطمورة. حيث طمرت العناقيد في مجال كولومي مضاءٍ و يقارب جهود مادلينج للبلورة التي تمت محاكاتها، و سُمح لأقرب الأيونات من هذه المراكز بالاسترخاء حتى الوصول إلى حالة اتزان جديدة. وقد أظهرت الحسابات النظرية لقيم Stokes shift أن توليد ضوء الليزر شديد التأثر بالعوامل المتزامنة التالية: حالات التأكسد للأيون الموجب الشائب، والدوال المتمركزة على موقع الفراغ الأنيوني لمركز التشوه. وأكدت النتائج أن جميع حالات الإثارة للأسطح المشوهة المسترخاة تقع على عمق أقل من الحواف السفلية لحزم التوصيل من المستوى الأرضي للأسطح الخالية من التشوه، مما يدعم إمكانية استخدام هذه المراكز كمراكز ليزر ملونة. وقد تم حساب طاقة الحاجز للتدمير الاتجاهي لهذه المراكز بسبب هجرة أيون البروميد من عمق بلورة بروميد الفضة إلى المراكز اللونيةF_A: Co^{+2}, Co^{+3}مما يؤدى إلى انطفاء في تجربة الليزر. وقد بينت النتائج أن التدمير الاتجاهي يتناسب تناسباً طردياً مع عدد تأكسد الأيون الموجب الشائب Co^{+2} <Co^{+3}. كذلك تم دراسة علاقة Glasner–Tompkins علي هذه المراكز الملونة وأظهرت النتائج أن تعمم هذه العلاقة لتشمل حالات التأكسد للأيون الموجب الشائب. وقد تناول هذا البحث محاولةً لتفسير دور هذه العوامل بدلالة جهد مادلينج، الميل الإلكتروني، كفاءة التحويل الضوئي – الضوئي، و الجهود الإلكتروستاتيكية بين السطح الماز و الجسيمات الممتزة.

و تم فحص إمكانية انتقال إلكترون من جزئ من الصبغات تحت تأثير Supersensitizer لقاع منطقة التوصيل لأسطح بروميد الفضة المحتوية علي المراكز الملونة F_A: Co^{+2}, Co^{+3}.وقد أوضحت النتائج زيادة الحساسية الفوتوغرافية لأسطح بروميد الفضة بزيادة حالات التأكسد للأيون الموجب الشائب.و قد تم إيعاز الاختلاف بين كفاءة الحساسية للصبغتين المدروستين في حالات الإثارة إلى الفروق بين مستويات أشباه فيرمي.